^{197}Au isomer-shift studies of charge-density perturbations in Au-based alloys

Paul G. Huray,* T. J. Kirthlink,† F. E. Obenshain, J. O. Thomson, and Cheng May Tung‡
Oak Ridge National Laboratory, Oak Ridge, Tennessee 37830§
and University of Tennessee, Knoxville, Tennessee 37916
(Received 12 April 1976)

Mössbauer spectra for ^{197}Au have been obtained for nominally 1-, 2-, and 4-at.% solid solutions of the elements Sc, Ti, V, Cr, Mn, Fe, Co, Ni, Cu, Zn, Ga, Ge, Ag, Cd, In, Sn, and Sb with high-purity gold at 4.2°K. The change in isomer shift from that of pure ^{197}Au arising from the charge-density perturbation by the impurity have been extrapolated to 0-at.% solute for these elements to determine the influence of impurities in gold upon the electronic conduction band. The resultant isomer shifts (corrected for volume effects) are presented in comparison to the residual electrical resistivity of the same impurities in gold and provide a new and more rigid constraint upon the character of the scattering potential at an impurity site in gold.

I. INTRODUCTION

When solute atoms are dissolved into a host metal (such as gold) a solid solution is said to be formed if the lattice structure (fcc for gold) of the resulting alloy is the same as that of the host metal. The limits of concentration of the solute material vary from vanishingly small to 100 at.%. In such a solid solution at 0 °K the solute atoms can be viewed as presenting a perturbing potential ΔV to electrons which otherwise see a perfectly periodic lattice of host potentials. The influence of the perturbing potential upon the host conduction band may alter the electronic structure in several ways. There will in general be local atomic distortions as well as an average lattice contraction (or expansion). Localized discrete bound states below the conduction band or virtual bound states with long-range screening may also result.

The perturbing potential will attract or repel electrons so as to provide screening in the region of the impurity. For sufficiently attractive ΔV, discrete localized bound states occur and for weaker perturbations, virtual bound states with energies lying within the conduction band occur. In this case Friedel charge oscillations surround the impurity and provide the screening charge. When larger solute concentrations are introduced, we may also measurably detect effects of multiple-scattering interactions, density-of-state changes, and elastic strains. These effects may be seen in the x-ray scattering, heats of formation, electrical resistivity, Knight shift, magnetic susceptibility, specific heat, and Mossbauer isomer-shift measurements.

We have in this study attempted to construct a set of gold solid-solution alloys which were dilute enough that the dominant effects on the electronic structure arise from single impurities. By extrapolation to zero solute concentration we, therefore, hope to reveal those effects in the electron charge-density distribution which would be produced by a single impurity (and its associated local distortion) in a one-to-one exchange with a gold atom in pure gold. However, account must be taken of the change in average charge density in the alloy arising from volume effects since a lattice expansion will in general decrease the amplitude of the electronic wave functions over the whole alloy. This lattice volume correction has been used in other alloy studies[1] and will be discussed below.

The ^{197}Au isomer shift depends on the charge density at the ^{197}Au nucleus. Thus, we picture the single impurity as producing a scattering center for the Au host conduction electrons which distribute themselves in a screening "cloud" about the scattering center and perhaps extend for many lattice spacings outward. This cloud of electrons is then an additional charge-density perturbation to that of pure-gold metal arising from the perturbation potential ΔV and increases or decreases the average electron charge density at the 12 near-neighboring gold nuclei, at the six second-near neighbors, and, etc. The gold near neighbors to such an impurity thus have a different Mössbauer isomer shift than do pure-metallic-gold nuclei. Since all near neighbors are equally radially displaced from the impurity we assume an equal influence at all 12, but allow the six second-near neighbors to have a yet different charge density and, etc., for the jth nearest-neighbor shells of atoms. The measurement of Mössbauer isomer shift for the solid-solution alloy is thus different from that of pure gold (after making volume corrections) by the influence of the average electron charge density scattered from the impurity to the various shells of gold neighboring atoms. Each shell of neighbors will then have its own characteristic isomer shift. However, the Mössbauer

linewidth is substantially greater than the typical isomer shift of the jth shell of neighbors and, therefore, discrete satellites are not resolvable.

The ^{197}Au Mössbauer isomer shift has been used for this work because it is particularly sensitive to small average charge-density changes at gold nuclei (often providing a sensitivity better than $\frac{1}{1000}$ of the normal 6s electron charge density at pure gold nuclei [$\rho_{Au}(0)$]).

II. EXPERIMENTAL MEASUREMENT PROCEDURE

The gold Mössbauer measurements reported here were made at 4.2 °K using a constant-acceleration electromechanical transducer. Data were collected in a multichannel analyzer operating in the multiscale mode. Sources of ^{197}Au γ rays were prepared by neutron activitation of platinum metal (enriched to 55-at.% ^{196}Pt) in the High Flux Isotope Reactor at the Oak Ridge National Laboratory. The ^{197}Pt β^- decays with an 18-h halflife through the 77.345-keV $\frac{1}{2}+$ first excited state of ^{197}Au to the $\frac{3}{2}+$ ground state. These γ rays provide the nuclear γ resonance used in the measurements. Typical count rates in this 77.345-keV line are $\sim 2\times 10^5$ counts/sec at the beginning of an experiment. The velocity scale was calibrated for each gold Mössbauer spectrum by simultaneously collecting a multiple-line ^{57}Fe spectrum for an Armco iron absorber at 296 ± 3 °K. The ^{57}Co source used to produce the ^{57}Fe γ rays was attached to the same drive rod which Doppler shifted the ^{197}Au γ rays and the two spectra were collected through a zero-dead-time dual-input multichannel scaling module. Because the ^{197}Pt source has only an 18-h halflife, the intensity of the 77.345-KeV γ rays were modulated by collimating them through a variable thickness of tin absorber. In this way the solid angle of the source–Ge(Li)-detector was maintained through the experiments while an approximately constant count rate of 10^5/sec was produced. Approximately 2×10^6 counts per channel were accumulated in 512 channels for each Mössbauer spectrum. A Gatling-gun absorber holder was employed so that we could rotate any of six absorbers into the collimated γ-ray beam without warming to room temperature. A pure-gold spectrum was always collected after a cool down to 4.2 °K followed by five alloy spectra and then another pure-gold spectrum before warm up. This procedure guaranteed a stability to our reference velocity scale and tended to eliminate any systematic electronic shifts in our apparatus.

Figure 1 shows a typical ^{57}Fe Mössbauer spectrum at the top, a pure-gold spectrum in the middle, and a ^{197}Au dilute alloy spectrum at the bottom. The ^{57}Fe spectrum was computer fit with a least-squares code of a Mössbauer transmission integral constrained to satisfy a magnetic Hamiltonian consisting of 15 absorption lines (of which only 11 are visible in the velocity range of Fig. 1). The pure-gold and alloy spectra were computer fit with the same code assuming a single unique line (i.e., unique charge density), but with variable linewidth to accommodate distributions which have a splitting which is small by comparison to a pure-gold linewidth. The zero of velocity as determined by the fitting of the top Fe spectrum is graphically superimposed on all spectra by means of the central vertical line. The isomer shift of the pure-gold absorber (relative to the gold in platinum source) is indicated by a second vertical line whose location was computer determined by the above code. The shift of this line ΔE from the zero of velocity is -1.223 ± 0.002 mm/sec. The isomer shift of the gold alloy absorber (relative to the gold in platinum source) is indicated by the third short vertical line whose location is again computer de-

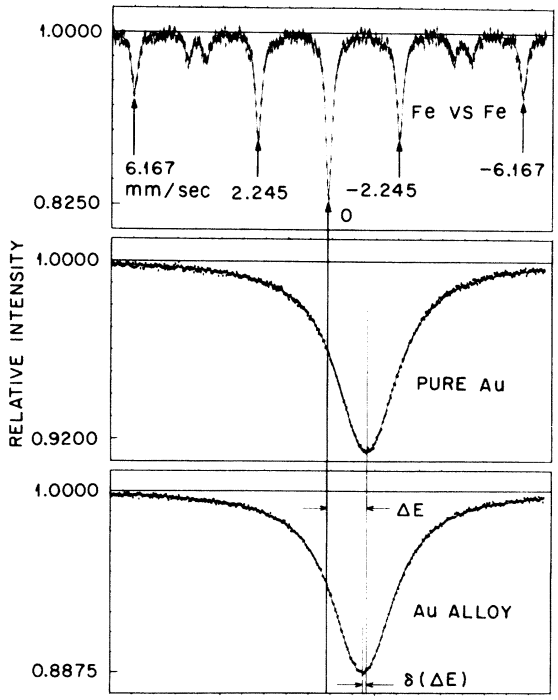

FIG. 1. Mössbauer spectra for (a) ^{57}Fe in Armco iron source with an Armco iron absorber at room temperature (top); (b) ^{197}Au at Pt source with a pure-gold absorber at 4.2 °K (middle); and (c) ^{197}Au in Pt source with nominal 4-at.%-Cd–96-at.%-Au alloy absorber at 4.2 °K (bottom). The isomer shift ΔE for ^{197}Au in Au vs ^{197}Au in Pt is indicated relative to the zero of velocity. $\Delta E = (v/c)77.345$ keV, where $v = -1.223 \pm 0.002$ mm/sec. $\delta(\Delta E)$ is the differential isomer shift of ^{197}Au in a gold alloy from that of pure gold.

termined. The shift of this line from the pure-gold-absorber isomer shift $\delta(\Delta E)$ is what we call the differential isomer shift and depends upon the product of the gold-nuclear-volume change during the γ-ray transition (assumed constant in this set of experiments) and the average electron charge density change at gold nuclei between the alloy and pure gold,[2] i.e.,

$$\delta(\Delta E) = k\frac{[\rho_{\text{alloy}}(0) - \rho_{\text{Au}}(0)]}{\rho_{\text{Au}}(0)} . \tag{1}$$

We have previously determined[2] the constant k to be ~8 mm/sec.

Samples were prepared by either induction melting or melting in a resistance furnace under an argon atmosphere. The correct weights of solute element were wrapped with 99.9999%-pure gold, heated to melting, and quenched into a water bath. For those solid solutions which remained stable at 700 °C a further anneal was carried out for 8 h after rolling to foil form. Actual composition of the calcium and scandium alloys were found by atomic-absorption measurements. All other compositions were determined by comparing the measurements of room-temperature residual electrical resistivity to the literature values of Linde[3] and assuming a $m(1-m)$ composition dependence. For those cases where the Mössbauer isomer shift and residual resistivity indicated a large discrepancy from nominal composition, x-ray analyses were also made. On this basis the results of the nominal 4-at.%-Ti, -Co, and -Mn gold alloys were rejected since all showed a partial non-solid-solution phase present in the sample.

III. MÖSSBAUER-ISOMER-SHIFT AND ELECTRICAL-RESISTIVITY MEASUREMENTS

In pure gold we have previously found[4] the Mössbauer isomer shift to depend upon the average volume per atom Ω as

$$\rho(0) = (\Omega_{\text{Au}}/\Omega)^{\gamma}\rho_{\text{Au}}(0), \tag{2}$$

where Ω_{Au} is the atomic volume per atom in normal uncompressed gold. The dependence was determined theoretically through a relativistic Wigner-Seitz Hartree Slater-Latter wave-function code. By computing $\rho(0)$ for several different atomic volumes near Ω_{Au}, γ was found to be approximately 0.86. Changes in $\rho(0)$ due to variations in Ω were found to be predominantly due to changes in the 6s wave function at the origin. However, the 0.86 power (rather than 1.0) can be ascribed to the screening effects of 5d electrons in the core which also depend upon Ω. The dependence [Eq. (2)] was also previously[1] experimentally verified through Mössbauer-isomer-shift measurements with pure gold at high pressures (up to 70 kbar) which produced changes in Ω up to $0.03\,\Omega_{\text{Au}}$.

We now assume as stated in the introduction that by adding to some of the gold atomic sites in the compressed (or expanded) lattice a perturbation potential ΔV, we can simulate the dilute alloy of interest. A perturbation calculation[5] (see also the following paper[6]) shows that the charge density at an average gold nucleus in a solid-solution alloy may be written as

$$\rho_{\text{alloy}}(0) = \left(\frac{\Omega_{\text{Au}}}{\Omega}\right)^{\gamma}\rho_{\text{Au}}(0)\left(1 + \frac{\langle\Delta\rho_{\text{sc}}(0)\rangle}{\rho_{\text{Au}}(0)}\right) \tag{3}$$

or

$$\rho_{\text{alloy}}(0) = \left(\frac{\Omega_{\text{Au}}}{\Omega}\right)^{\gamma}\rho_{\text{Au}}(0)\left(1 + \sum_{j=1}^{\infty}\langle n_j\rangle\frac{\Delta\rho_{\text{sc}}(r_j)}{\rho_{\text{Au}}(0)}\right) . \tag{4}$$

Here $\langle\Delta\rho_{\text{sc}}(0)\rangle/\rho_{\text{Au}}(0)$ is the average fractional change in charge density at an alloy gold nucleus brought about by scattering from foreign (solute) atoms in the alloy, $\langle n_j\rangle$ is the average number of foreign atoms in the jth shell of neighbors to the gold atom at $r=0$, and $\Delta\rho_{\text{sc}}(r_j)/\rho_{\text{Au}}(0)$ is the fractional scattered charge density (screening cloud) associated with the perturbation ΔV located at a point r_j away from $r=0$. A choice of the form ΔV leads to a theoretical value for this scattered charge density distribution as shown in the following paper.[6]

For an alloy with no short-range order (the random distribution of solute atoms of an fcc lattice), $\langle n_j\rangle = mc_j$, where m is the atomic fraction of solute atoms in the alloy and c_j is the total number of atoms in the jth shell of neighbors ($c_1=12, c_2=6, \ldots$). Combining Eqs. (1) and (4) we see that the differential Mössbauer isomer shift $\delta(\Delta E)$ is given by

$$\delta(\Delta E) = k\left\{\left(\frac{\Omega_{\text{Au}}}{\Omega}\right)^{\gamma}\left[1 + \left(\sum_{j=1}^{\infty}c_j\frac{\Delta\rho_{\text{sc}}(r_j)}{\rho_{\text{Au}}(0)}\right)m\right] - 1\right\} \tag{5}$$

within the model approximations. By measuring $\delta(\Delta E)$ vs m (nominally +0.01, 0.02, and 0.04) for the solid = solution alloys of gold with Sc, Ti, V, Cr, Mn, Fe, Co, Ni, Cu, Zn, Ga, Ge, Ag, Cd, Sn, and Sb, and correcting for volume [as in Eq. (5)] we may determine $\sum_{j=1}^{\infty}c_j\Delta\rho_{\text{sc}}(r_j)/\rho_{\text{Au}}(0)$ for each of these foreign atoms in gold. Our sensitivity gives this value to better than $\frac{1}{1000}$ of the charge density of 6s electron at pure-gold nuclei, $\rho_{\text{Au}}(0)$.

The systematic variation of $\delta(\Delta E)$ with alloy composition m for these impurities is given in Table I. We see that the differential isomer shift $\delta(\Delta E)$ is very nearly linearly dependent upon solute or impurity concentration [as predicted by

TABLE I. Variation of $\delta(\Delta E)$ with alloy composition.

Solute	at.%	Differential isomer shift $\delta(\Delta E)$ (mm/sec)	Residual resistivity $1/\sigma$ ($\mu\Omega$ cm) $T=300$ °K	$T=78$ °K	$T=4.2$ °K	$\frac{\delta a}{a}$ (per at.%)
Ca	0.87		0.678	0.465	0.347	
Sc	0.54	0.059 ± 0.010	5.183	5.083	4.964	0.000 855
	1.30	0.143 ± 0.010	11.288	11.252	11.137	
	2.32	0.308 ± 0.010	21.877	22.080	21.962	
Ti	0.98	0.075 ± 0.010	12.602	12.284	12.084	−0.0259
	1.64	0.163 ± 0.010	20.984	20.928	20.817	
V	0.97	0.059 ± 0.010	11.265	12.569	13.020	−0.000 298
	2.27	0.120 ± 0.010	26.050	29.440	30.974	
	4.73	0.292 ± 0.010	52.852	58.686	61.244	
Cr	0.89	0.049 ± 0.010	3.778	4.205	4.068	−0.000 548
	1.72	0.073 ± 0.010	7.236	7.783	7.264	
	3.86	0.210 ± 0.010	15.932	16.455	15.306	
Mn	0.88	0.045 ± 0.010	2.131	2.197	2.144	−0.000 178
	2.10	0.076 ± 0.010	5.002	5.099	4.876	
Fe	1.01	0.039 ± 0.010	7.991	8.078	7.806	−0.000 662
	2.29	0.110 ± 0.010	17.858	18.083	17.483	
	3.47	0.170 ± 0.010	26.693	26.908	26.095	
Co	1.17	0.045 ± 0.010	6.139	6.407	6.606	−0.000 841
	2.31	0.109 ± 0.010	12.035	12.913	13.520	
Ni	1.23	0.038 ± 0.010	0.967	0.897	0.865	−0.000 731
	2.23	0.079 ± 0.010	1.743	1.591	1.538	
	4.26	0.177 ± 0.010	3.257	3.035	2.958	
Cu	0.92	0.033 ± 0.002	0.413	0.422	0.418	−0.000 927
	1.71	0.069 ± 0.002	0.762	0.788	0.773	
	3.74	0.162 ± 0.002	1.683	1.627	1.597	
Zn	0.89	0.040 ± 0.002	0.849	0.825	0.796	−0.000 46
	1.89	0.076 ± 0.002	1.780	1.771	1.770	
	3.78	0.148 ± 0.002	3.491	3.325	3.273	
Ga	0.82	0.023 ± 0.002	1.800	1.740	1.693	−0.000 144
	1.17	0.046 ± 0.002	2.563	2.209	2.127	
Ge	0.36	0.018 ± 0.002	1.883	1.641	1.492	0.000 185
	0.58	0.034 ± 0.002	3.002	2.693	2.503	
Ag	0.98	0.027 ± 0.002	0.351	0.362	0.358	−0.000 021
	1.86	0.041 ± 0.002	0.664	0.676	0.666	
	3.64	0.082 ± 0.002	1.274	1.294	1.271	
Cd	1.01	0.025 ± 0.002	0.633	0.607	0.595	0.000 438
	2.06	0.063 ± 0.002	1.282	1.212	1.174	
	3.79	0.112 ± 0.002	2.319	2.248	2.237	
In	0.95	0.029 ± 0.002	1.324	1.272	1.239	0.000 686
	1.83	0.054 ± 0.002	2.519	2.425	2.424	
	3.59	0.103 ± 0.002	4.863	4.645	4.531	
Sn	0.93	0.014 ± 0.002	3.125	2.962	2.939	0.000 959
	1.82	0.044 ± 0.002	6.053	5.873	5.783	
	3.65	0.062 ± 0.002	11.950	11.642	11.482	
Sb	0.47	0.020 ± 0.002	3.219	2.990	2.822	0.001 154

Eq. (5)] for every alloy studied. Note that several 4 at.%-alloy data points were not included in these figures due to a low solubility limit.

Through the volume correction expressed in Eq. (5) and a least-squares fit to the data of Table I by a linear function of m we may obtain a value for $\sum_{j=1}^{\infty} c_j \Delta\rho_{sc}(r_j)/\rho_{Au}(0)$, the total scattered charge density change brought about at the gold nuclei located at r_j due to the screening cloud of electrons associated with the impurity located at $r=0$. We see that these volume corrected slopes depend upon the type of impurity introduced and we have chosen to display this variation in Fig. 2 as a function of nominal $Z = Z_{\text{impurity}} - Z_{\text{gold}}$. Here Z_{impurity} is the number of electrons outside a free-atom closed shell and $Z_{\text{gold}} = 1$.

For reference we also show in Fig. 3 the lattice parameter $\Delta a/a$ per at.% for the alloys due to different atomic sizes of gold and solute atoms. The values shown in Fig. 3 and reported in Table I are from the Pearson[7] tables with the exception of the value of Sc in Au which we have measured. In Fig. 4 we indicate the influence of the conduction-electron scattering at the Fermi level by plotting the residual electrical resistivity of 1% of these impurities also as a function of the parameter ΔZ. The solid lines connect the residual electrical resistivity per at.% for measurements at $T \simeq 300\ ^{\circ}\mathrm{K}$ as determined by Johansson and Linde.[3] The experimental values of $1/\sigma$ given in Table I have been used in every case except for the calcium and scandium alloys to determine actual alloy composition based upon the literature values of Johansson and Linde.[3] Figure 4 also shows the limiting values of residual electrical resistivity as T approaches $0\ ^{\circ}\mathrm{K}$.[8] The $1/\sigma$ and $\delta a/a$ values given in Table I and shown in Figs. 3 and 4 for scandium are (as far as we are aware) the first reported. The $1/\sigma$ value for Ca has been placed in Fig. 4 to denote its minimum value only since x-ray results show the alloy not to be a complete solid solution.

The perturbation potential ΔV which is chosen to simulate the pure-metal potential with one impurity at $r=0$ must produce a differential scattered charge-density distribution which is consistent with the measured electrical resistivity and with the requirement of electrostatic screening. The distribution will have contributions from all

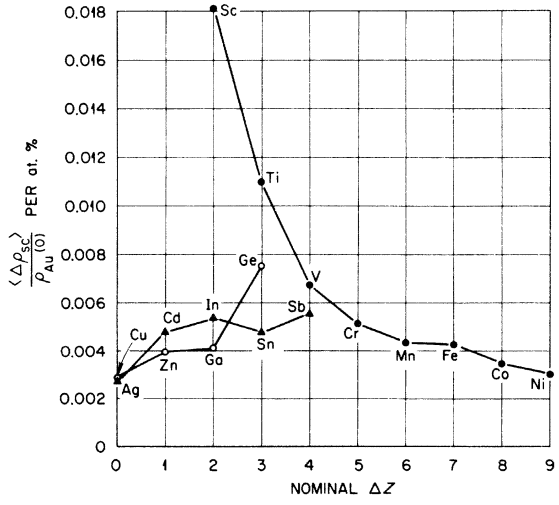

FIG. 2. Average scattered charge density per at.% solute from impurities in the gold lattice as measured at neighboring gold nuclei. The values are reported as a fraction of $\rho_{Au}(0)$, the conduction-electron charge density at the average gold nuclei in pure gold.

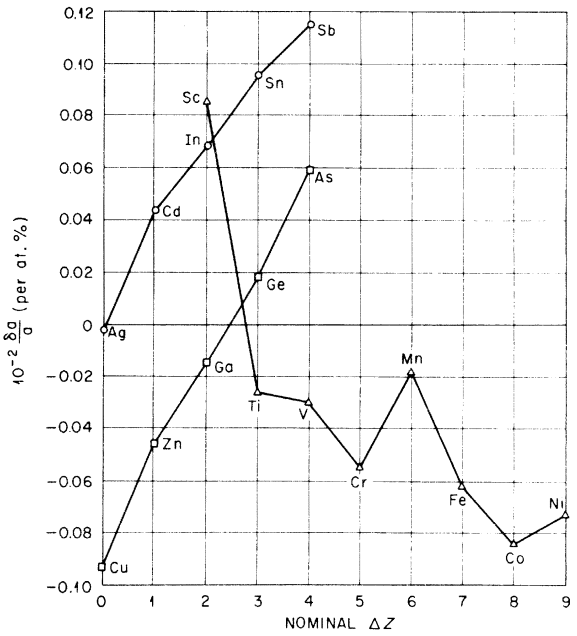

FIG. 3. Relative lattice parameter change per at.% of concentration for impurities in gold. The data are presented as a function of nominal $Z = Z_{\text{impurity}} - Z_{\text{gold}}$.

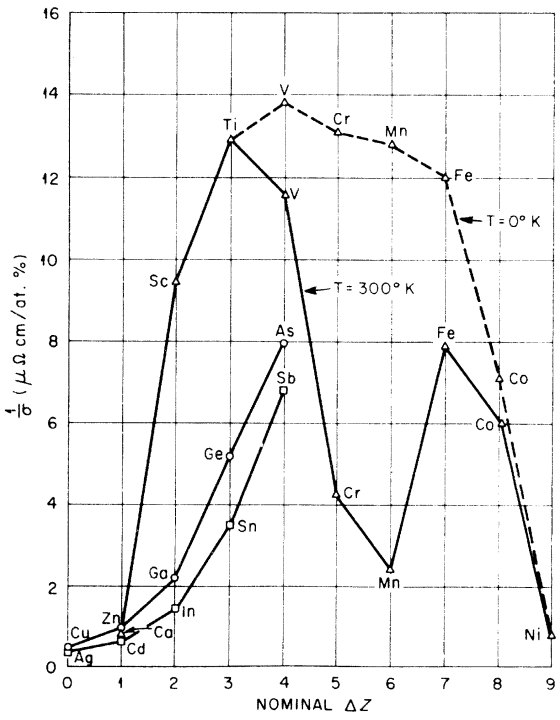

FIG. 4. Residual electrical resistivity per at.% of solute concentration for several impurities in gold.

levels within the conduction band and may not, therefore, behave in the same manner as the residual resistivity which is dominantly dependent upon the Fermi level character. The perturbation ΔV will also produce Mössbauer-isomer-shift effects which are sampled at all radii in a non-negligible manner. In this sense the experimental measure of $\sum_{j=1}^{\infty} c_j \Delta\rho_{sc}(r_j)/\rho_{Au}(0)$ places a new and more rigid constraint upon the character of the scattering potential at the impurity site.

---

*Supported partially with funds provided by a Research Corporation Grant.

†Work performed in partial fulfillment of the degree of Master of Science in Physics at the University of Tennessee. Present Address: Oak Ridge Technical Equipment Company, Oak Ridge, Tenn. 37830.

‡Work performed in partial fulfillment of the degree of Doctor of Philosophy in Physics at Louisiana State University.

§Work support by Union Carbide Corp. under contract with U. S. Energy Research and Development Administration.

[1]Louis D. Roberts, D. O. Patterson, J. O. Thomson, and R. P. Levey, Phys. Rev. 179, 656 (1969).

[2]Louis D. Roberts, Richard L. Becker, F. E. Obenshain, and J. O. Thomson, Phys. Rev. 137, A895 (1965).

[3]C. H. Johansson and J. O. Linde, Ann. Phys. 25, 17 (1936).

[4]Thomas C. Tucker, Louis D. Roberts, C. W. Nestor, Jr., and Thomas A. Carlson, Phys. Rev. 178, 998 (1969).

[5]Paul G. Huray, Louis D. Roberts, and J. O. Thomson, Phys. Rev. B 4, 2147 (1971).

[6]Paul G. Huray, Cheng May Tung, F. E. Obenshain, and J. O. Thomson, Phys. Rev. B (to be published).

[7]W. B. Pearson, *The Crystal Chemical and Physics of Metals and Alloys* (Wiley, New York, 1972).

[8]A. J. Heeger, Solid State Phys. 23, 283 (1969).